GCAGS JOURNAL
A Publication of the Gulf Coast Association of Geological Societies
www.gcags.org

Using Fault Kinematics to Evaluate the Relationship between Cenozoic Fault Activity, Sedimentation Rates, and Salt Movement in the Gulf of Mexico: A Comparison between Southwestern and Southeastern Louisiana

Abah P. Omale and Juan M. Lorenzo

Department of Geology and Geophysics, Louisiana State University, E235 Howe-Russell Bldg., Baton Rouge, Louisiana 70803, U.S.A.

ABSTRACT

Fault initiation and reactivation across southern Louisiana during the Cenozoic was driven by either clastic sediment progradation mobilizing underlying salt or by sediment progradation inducing tensional bending stresses during lithospheric flexure. Climate and tectonics within the North American continent during the Cenozoic created differences in the source location, amount of sediments transported, as well as the spatial and temporal distribution of sediments transported into the Gulf of Mexico. This study analyzes 140 fault intercepts along eleven regional cross sections containing well log data in southern Louisiana. Cumulative throw, incremental throw, and fault slip rates indicate fault activity punctuated by periods of fault inactivity in southwestern and southeastern Louisiana. Results show a correlation between the timing of fault reactivation and the location of sediment depositional centers in the Cenozoic. In southwestern Louisiana and southeastern Louisiana faulting increases significantly in the Oligocene–Early Miocene and Early Miocene, respectively, during the emergence of new depositional centers in these areas. The pattern of fault activity correlates with the pattern of sediment deposition by showing a similar shift in major activity from southwestern to southeastern Louisiana through time. The Eocene period marks a time when most faults in southwestern and southeastern Louisiana were inactive, possibly because the sediment depositional center existed in central Louisiana. These data show that the timing of fault activity correlates with the timing of sediment loading and salt movement as opposed to lithospheric flexure in the Cenozoic.

INTRODUCTION

Fault initiation and reactivation have been documented in the southern Louisiana portion of the Gulf of Mexico in the Cenozoic (Thorsen, 1963; Hanor, 1982; Lopez, 1990; Heinrich, 2000; Al Dhamen, 2014). The cause of fault activity has been attributed to either salt movement ('salt tectonics model' or lithospheric flexure ('lithospheric flexure model') caused by the weight of prograding Cenozoic clastic sediments because the timing of fault reactivation correlates with the timing of sediment deposition, salt movement and predicted lithospheric flexure (Nunn, 1985; Diegel et al, 1995; Peel et al., 1995; McBride, 1998).

Manuscript received April 1, 2015; revised manuscript received June 8, 2015; manuscript accepted June 25, 2015.

GCAGS Journal, v. 4 (2015), p. 132–146.

This study involves the kinematic analysis of faults (Cartwright et al., 1998) from well log data across southwestern and southeastern Louisiana. The aim of this study is to understand the major driving mechanism for fault reactivation in southern Louisiana. In addition, this work will determine the amount and timing of fault reactivation and also provide a better understanding of the spatial distribution of fault reactivation in southwestern Louisiana and southeastern Louisiana. Furthermore, this study also compares the faulting history between southwestern and southeastern Louisiana to provide a better understanding of the interaction among Cenozoic fault activity, sediment loading, salt movement or lithospheric flexure.

Two major models exist to explain the cause of faulting in the Gulf of Mexico. The first model is related to salt tectonics (Worrall and Snelson, 1989; Diegel et al., 1995; Peel et al., 1995; Schuster, 1995; Vendeville, 2005). In this model, salt flows through differential loading and gravity spreading. Differential loading by sediments causes salt to flow in response to the difference in load caused by a seaward thinning wedge of sediment. As a result the salt moves laterally and vertically inducing normal

faulting in overlying sediments. During gravity spreading, the unstable slope of a sediment wedge causes the sediment to spread over the underlying weak salt layer (Vendeville, 2005). Spreading results in a proximal extensional region where the sediment overburden deforms through normal faulting, a middle translation region where the sediment overburden is translated seaward, and a distal region where the sediment overburden deforms by contraction in the form of folding or thrusting (Vendeville, 2005). Within these models, the regions of extension and contraction are translated seaward during clastic sediment progradation, such that a zone of contraction previously overlain by the distal and less dense part of the sedimentary wedge can become an extensional zone if loaded by a thicker and denser part of the sedimentary wedge (Vendeville, 2005).

Fault initiation and reactivation can also occur as a result of tensional bending stresses acting on the lithosphere—'lithospheric flexure model' (Nunn, 1985). This second model suggests that the southern Louisiana portion of the Gulf of Mexico is currently in a tensional state of stress at the periphery of the Pleistocene depositional center. Rapid sedimentation rates (1.2–1.8 mm/yr) allow for these stresses to accumulate and reactivate pre-existing growth faults (Nunn, 1985).

Different sources of sediment, fluvial/deltaic axes and depositional centers affected the sedimentation in the Gulf Coast at different times in the Cenozoic (Galloway et al., 2011). The Cenozoic depositional pattern of the Gulf Coast shows progradation of the shelf margin basinward with time (Winker, 1982). Eight fluvial/deltaic axes supplied sediments to the northern Gulf of Mexico throughout the Cenozoic (Galloway et al., 2011). Three of these principal fluvial/deltaic axes affected southern Louisiana, namely the Red River, the ancestral Mississippi River, and the ancestral Tennessee River (Galloway et al., 2000, 2011; Combellas-Biggot and Galloway, 2006) (Fig. 1).

The time when each of these fluvial/deltaic depositional centers was most active in the Cenozoic reflects a shift in the axes of deposition from west to east and back to the west (Woodbury et al., 1973; Galloway et al., 2000) (Fig. 1). The shifting depositional center timing and location are the result of tectonic and climatic changes occurring in the North American continent. These tectonic and climatic forces are associated with the late Laramide orogeny, Basin and Range extension, and regional crustal heating, volcanism, uplift, erosional unroofing of the Appalachians Mountains and epeirogenic uplift of the Rocky Mountains at different times in the Cenozoic. These tectonic and climatic changes converted topographic lows to highs and previous uplands to low lands in addition to influencing the amount of runoff available to transport sediment. Consequently, these forces controlled the amount and location of sediments brought into southwestern and southeastern Louisiana by controlling the location of sources, amount of runoff available to transport sediment, location of drainages, and amount of sediment transported, making the amount of Cenozoic sediment deposition differ in time and space (Galloway et al., 2000, 2011; Combellas-Biggot and Galloway, 2006) (Fig. 1). This difference also implies a difference in the timing and amount of fault reactivation, salt movement and lithospheric flexure due to sediment loading.

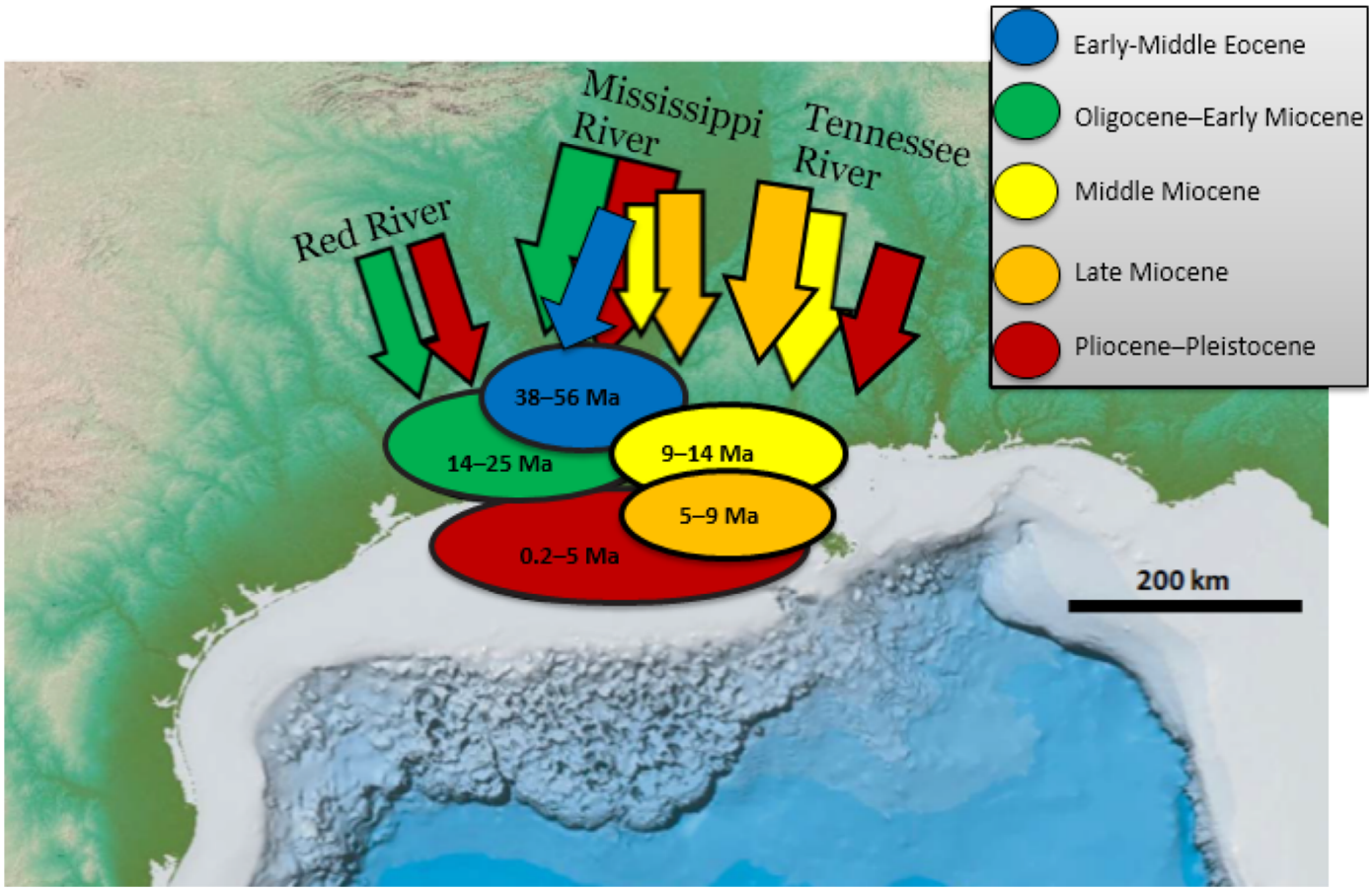

Figure 1. Cenozoic onshore locations of sediment depositional centers in southern Louisiana (modified after Al Dhamen [2014], Galloway et al. [2001, 2011], Combellas-Biggot and Galloway [2006], and Woodbury et al. [1973]). Three main rivers/fluvial axes were active. The width of the ellipses represents approximate longitudinal extent while the height of the ellipses represents the approximate latitudinal extent of the major depositional area. Note, however, that the latitudinal extent of the major depositional area is approximately the same for the Middle Miocene and Late Miocene.

DATA AND METHODS

Kinematic analysis of faults involves measuring the apparent cumulative throw across faults and making graphical plots of apparent cumulative throw versus depth in the hanging-wall block (T–Z) and calculated throw versus time (ΔT–t) (Mansfield and Cartwright, 1996; Cartwright et al., 1998; Castelltort et al., 2004) in order to study the Cenozoic fault activity in southwestern and southeastern Louisiana.

Faults originally identified (Bebout and Gutierrez, 1982, 1983) and verified by this study were analyzed in well log data along eleven regional cross sections in order to define the structure and stratigraphy in the study area (Bebout and Gutierrez, 1982, 1983) (Fig. 2). Six of these regional cross sections are across southwestern Louisiana and the other five are across southeastern Louisiana along strike and dip. These cross sections are structural cross sections and comprise 150 correlated and interpreted spontaneous potential and resistivity logs containing dated stratigraphic horizons with ages constrained by biostratigraphy from within the Cenozoic depositional centers in southern Louisiana. Additional well logs were correlated in this study in order to verify the structure and stratigraphy defined in the regional cross sections. Well logs (Drilling Info Inc.) were displayed using Geographix software (LMKR, 2014). The stratigraphic intervals on the well logs and cross sections, as defined by lithostratigraphic and biostratigraphic relations, are the major formations in Louisiana (Bebout and Gutierrez, 1982, 1983) (Fig. 3).

The well logs used in this study do not sample depths shallower than 3000 ft. For this study, the twelve Cenozoic stratigraphic horizons are listed from the youngest to the oldest and the numerical age of each formation top is assumed to correlate with published chronostratigraphic ages for that formation (Hackley, 2012) (Fig. 3).

Furthermore, this study also involves the analysis of 140 fault intercepts from within these regional cross sections (Fig. 2). Eighty-six of these faults are from southwestern Louisiana and the other 54 from southeastern Louisiana. Vertical separation, a quantification of fault displacement as the vertical distance between a horizon and its offset equivalent as projected across the fault for normal faults, was determined for these faults at multiple horizons directly from the cross sections, and correspond well to measured missing sections from well log correlation and analysis. Although we technically measured vertical separations, we use herein "throw" to describe the displacement because vertical separation and throw are nearly equal due to the relatively low dip exhibited by the strata (Tearpock and Bischke, 2003).

To define periods of fault activity using the ΔT–t and T–Z plot methods, we apply the 'fill to the top assumption' where we assume that the sedimentation keeps up with subsidence and accommodation creation, leaving no persistent fault scarp after the deposition of sediments at any given time (Mansfield and Cartwright, 1996; Castelltort et al., 2004). In addition, there is also the assumption that no significant erosion occurs on the hanging-wall block or the footwall block to affect measured throw values.

With the 'fill to the top assumption,' any throw experienced by a stratigraphic interval is defined as post-depositional and the difference in throw between two time periods can be calculated by subtracting the throw of all the younger intervals from the older interval. With this assumption also, any increase in throw (ΔT) with depth (Z) at any time (t) can be defined as a period of fault activity. Positive slopes in the T–Z plot are defined as periods of fault activity whereas periods of no slope (ΔT/ΔZ = 0) represent periods of fault inactivity. If the 'fill to the top assump-

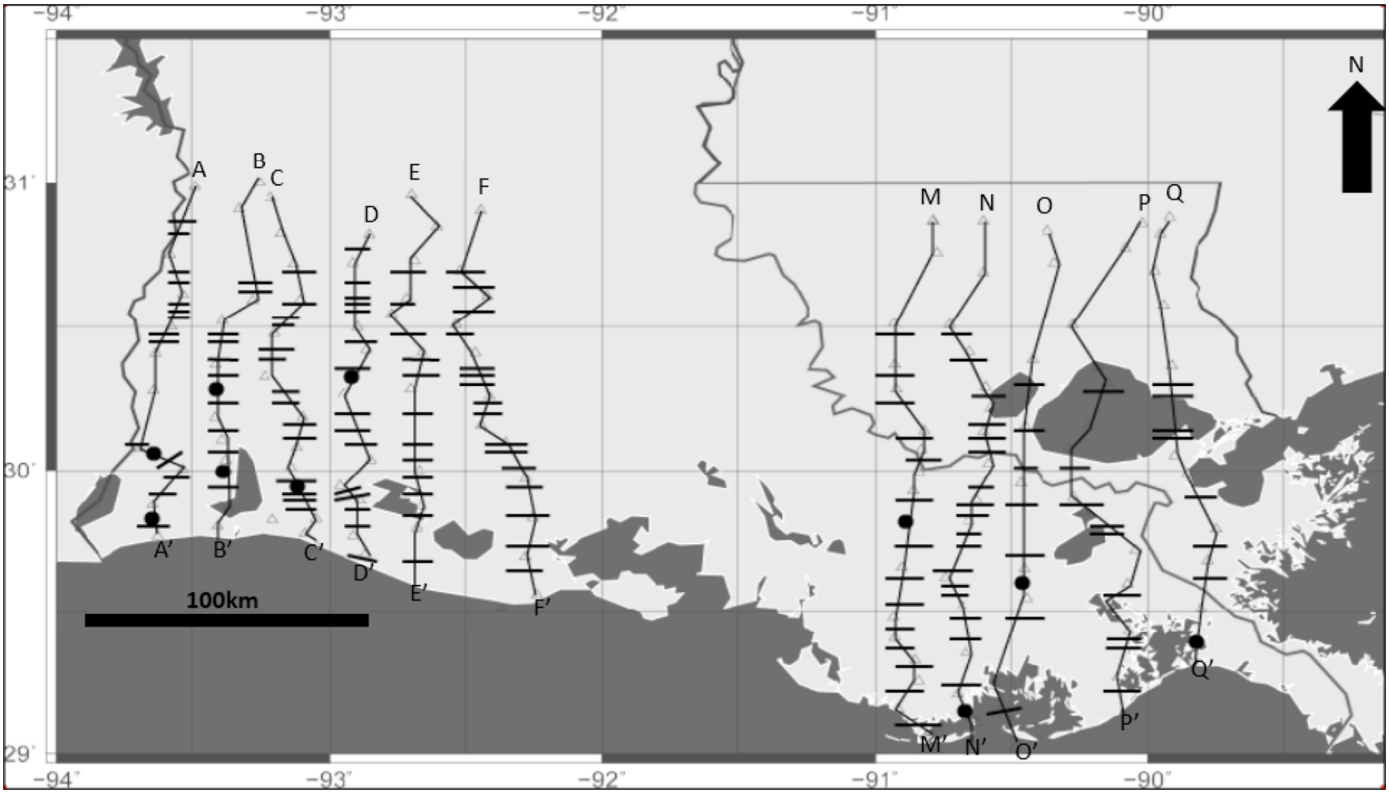

Figure 2. Regional cross sections used in this study. Cross sections are labelled A–A' through F–F' for southwestern Louisiana and M–M' through Q–Q' for southeastern Louisiana. Small triangles represent some of the wells used in the cross sections. Horizontal lines of all lengths represent faults identified (Bebout and Guttierez, 1982, 1983; this study) in the cross sections between the wells, and black circles represent salt domes (modified after Bebout and Gutierrez, 1982, 1983). The faults herein are numbered sequentially from north to south when presented in the tables (Appendix).

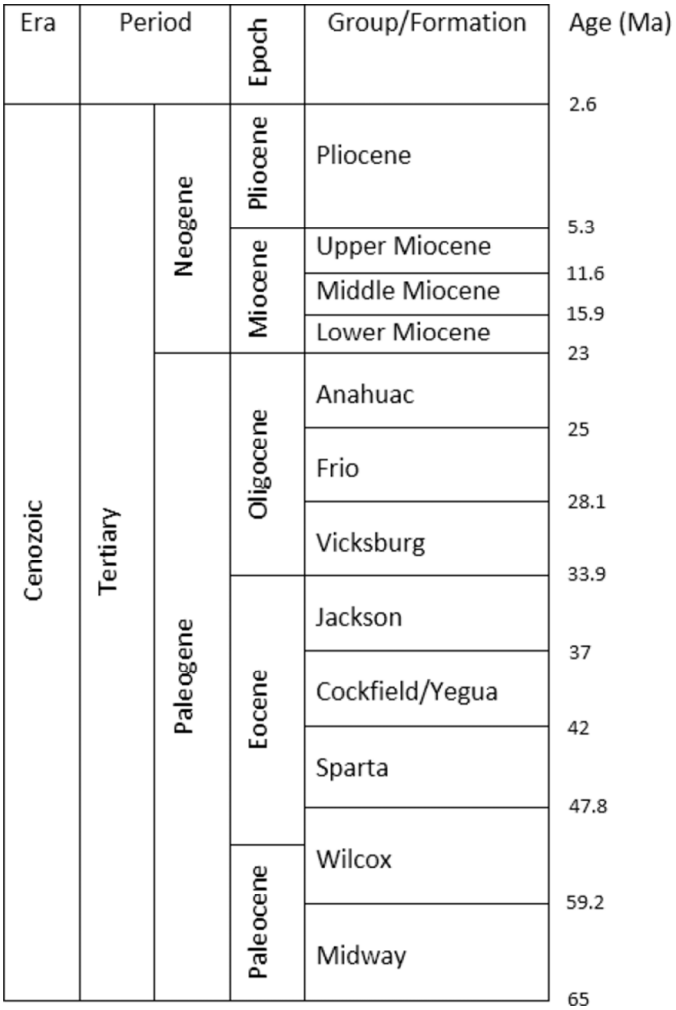

Figure 3. Ages of formation and other sediment unit tops used in this study to correlate well logs in the regional cross-sections A–A' through F–F' and M-M' through Q-Q' (modified after Bebout and Gutierrez [1982, 1983] and Hackley [2012]).

tion' does not hold and there is the preservation of fault scarp, then a period of actual fault activity may be defined as a period of apparent fault inactivity as in the case of pelagic sedimentation depositing equal thickness on both the hanging-wall block and footwall block during fault growth (Cartwright et al., 1998).

Also if the fault scarp is preserved, and there is deposition of different sediment thicknesses on both hanging-wall block and footwall block, a period of actual inactivity may be defined as a period of apparent fault activity whereas it only represents a filling of the previously generated fault topography. Differential erosion may also occur when a fault scarp is preserved and sediments from the footwall block are eroded and transported onto the hanging-wall block. Reduction of the thickness in the footwall block will lead to a reduction in the measured fault displacement values.

Slip rates of horizon tops through time were calculated and compared with calculations of decompacted one-dimensional sedimentation rates. The sedimentation rates were calculated from measured sediment thicknesses along the regional cross sections in order to determine the relationship between changes in depositional location, sedimentation rates, and changes in fault motion. The data are also presented as plots comparing slip rates and sedimentation rates between southwestern and southeastern Louisiana. The slip rates were calculated by dividing the throw at each time period by the numerical age for the same period.

The sediment decompaction was done in order to give estimates of the original thickness of sediment deposited by accounting for porosity loss during sediment burial. Sediment was decompacted using a decompaction software program, Flex-De-Comp™ (Kusznir et al., 1995). In decompaction, grain size is important because shales compact more than sandstones during burial (Allen and Allen, 2006). In this study, the decompaction was done by assuming a silt grain size for the entire section. Electric log patterns for the eleven cross sections show alternations of sand and clays within a particular formation with the wells showing nearly equal thickness of sand and clay. Consequently, although the use of silt-sized particles for the decompaction may cause some errors, the errors were minimized by using an intermediate grain size and by also using the same grain size for all the sections. Sedimentation rates were obtained following decompaction by dividing the original thickness of sediments by the numerical duration of its corresponding formation. Finally, interpretations of a major driving mechanism were made from the results by checking for correlations with model predictions of salt movement or lithospheric flexure.

RESULTS

Fault Kinematics in the Cenozoic of Southwestern Louisiana

The kinematics of 86 faults from southwestern Louisiana are presented herein. These faults are numbered in increasing order from north to south (Figs. 2 and 4–8; Appendix). These faults record the fault slip history throughout the Cenozoic Era. The measured apparent cumulative stratigraphic throw for 72 faults show fault activity from the Paleocene to the Pliocene as defined by increase in throw with depth. The measurements of cumulative throw-versus-depth also define periods of fault inactivity in fourteen faults by showing no change in cumulative throw with depth (Fig. 6; Appendix). The measurements of the incremental throw-versus-time for the same faults also confirm the increment in throw of a single horizon through time (Fig. 5; Appendix). The results of incremental throw at each time for these 14 faults constrain the periods of inactivity to within the Eocene (Fig. 7; Appendix). The maximum throw in the faults is in the Early Miocene; however, the maximum incremental throw across a particular formation top tends to increase along most of the different faults in a basinward direction (Appendix).

Calculated incremental throw and average slip rates show five-fold increase in the Late Oligocene–Early Miocene (Tables 1 and 3; Fig. 8; Appendix) and calculated average sedimentation rates are highest in the Oligocene (Table 2). These maximum slip rates and sedimentation rates represent relatively high values for the Gulf Coast.

Fault Kinematics in the Cenozoic of Southeastern Louisiana

The 54 faults studied in southeastern Louisiana record their fault slip history during the Cenozoic. These faults are numbered in increasing order from north to south (Figs. 2 and 8–12; Appendix). The measurements of the apparent cumulative stratigraphic throw-versus-depth for 47 faults show fault reactivation from the Paleocene to the Pliocene (Figs. 9–12; Appendix). The other seven faults studied indicate periods of fault reactivation punctuated by periods of inactivity (Figs. 11 and 12; Appendix). Incremental throw-versus-time calculations imply that the timing of fault reactivation occurs between the Paleocene through the Pliocene on 48 faults (Appendix). The calculations also show periods of inactivity were during the Eocene, Oligocene, Early Miocene, and Late Miocene (Appendix). However, most of the fault inactivity was during the Eocene (Fig. 12; Appendix). The maximum incremental throw occurs during the Late Miocene. The

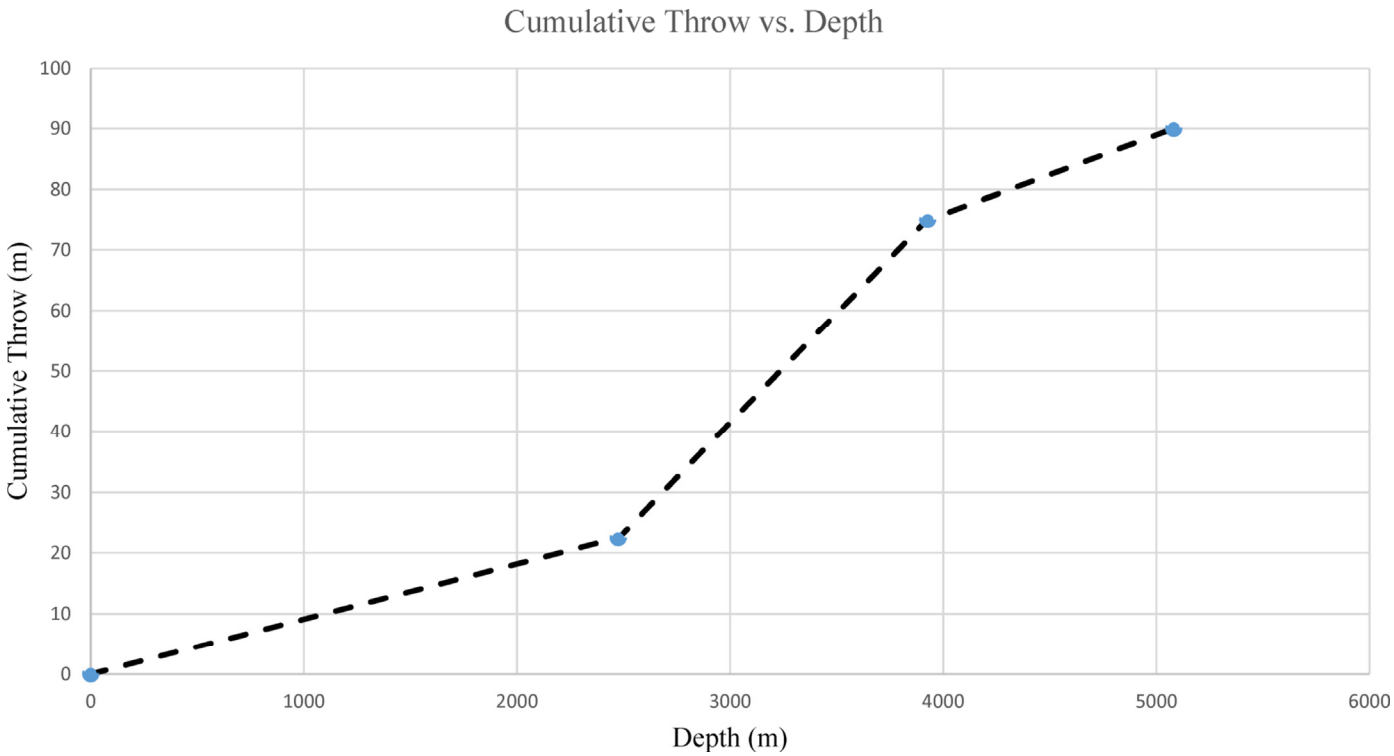

Figure 4. T–Z plot for fault 12 along regional cross-section C–C' (Appendix) showing cumulative throw of 90 m. Positive slopes indicate continuous fault reactivation. Dots represent values of cumulative throw and depth of formation tops in the hanging-wall block.

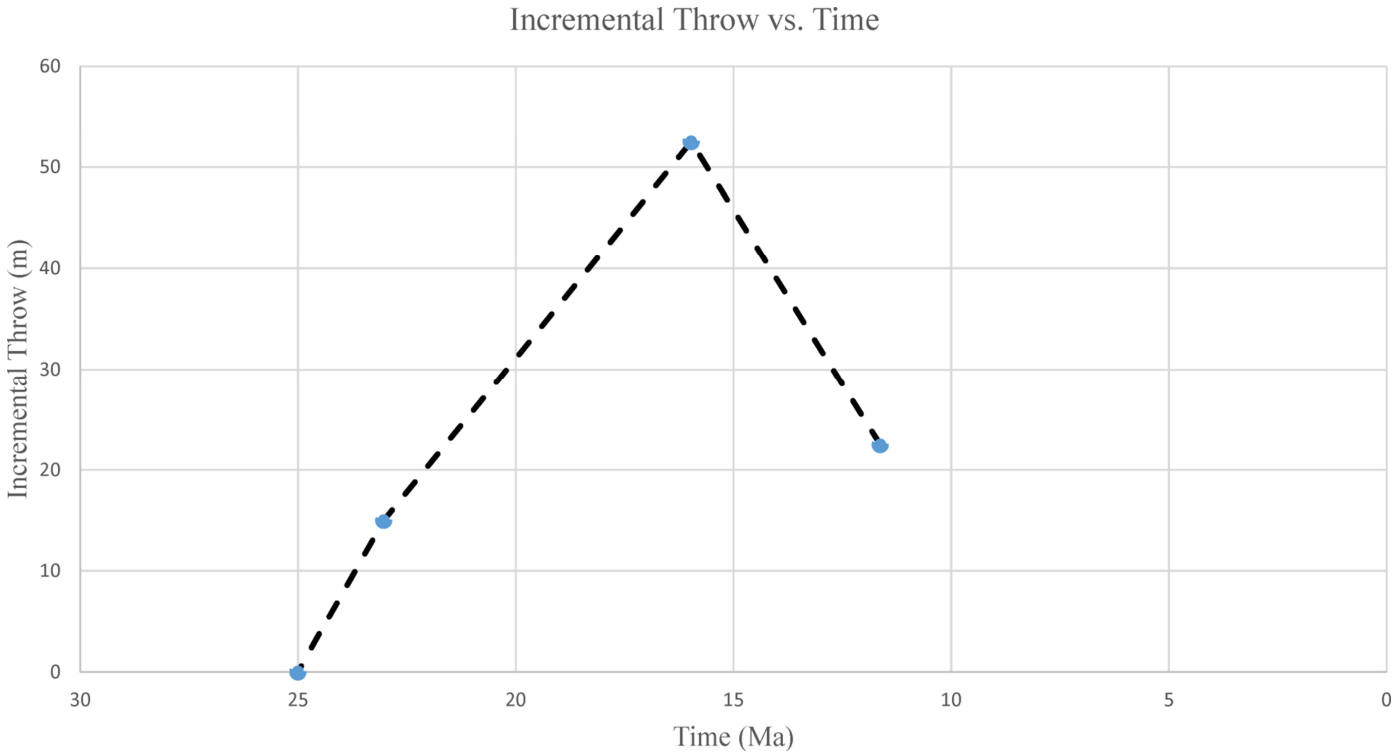

Figure 5. ΔT–t plot for the same fault in Figure 4 above showing increase in throw in the Oligocene and Miocene (25–11.6 Ma). Maximum incremental throw of ~53 m in the Lower Miocene.

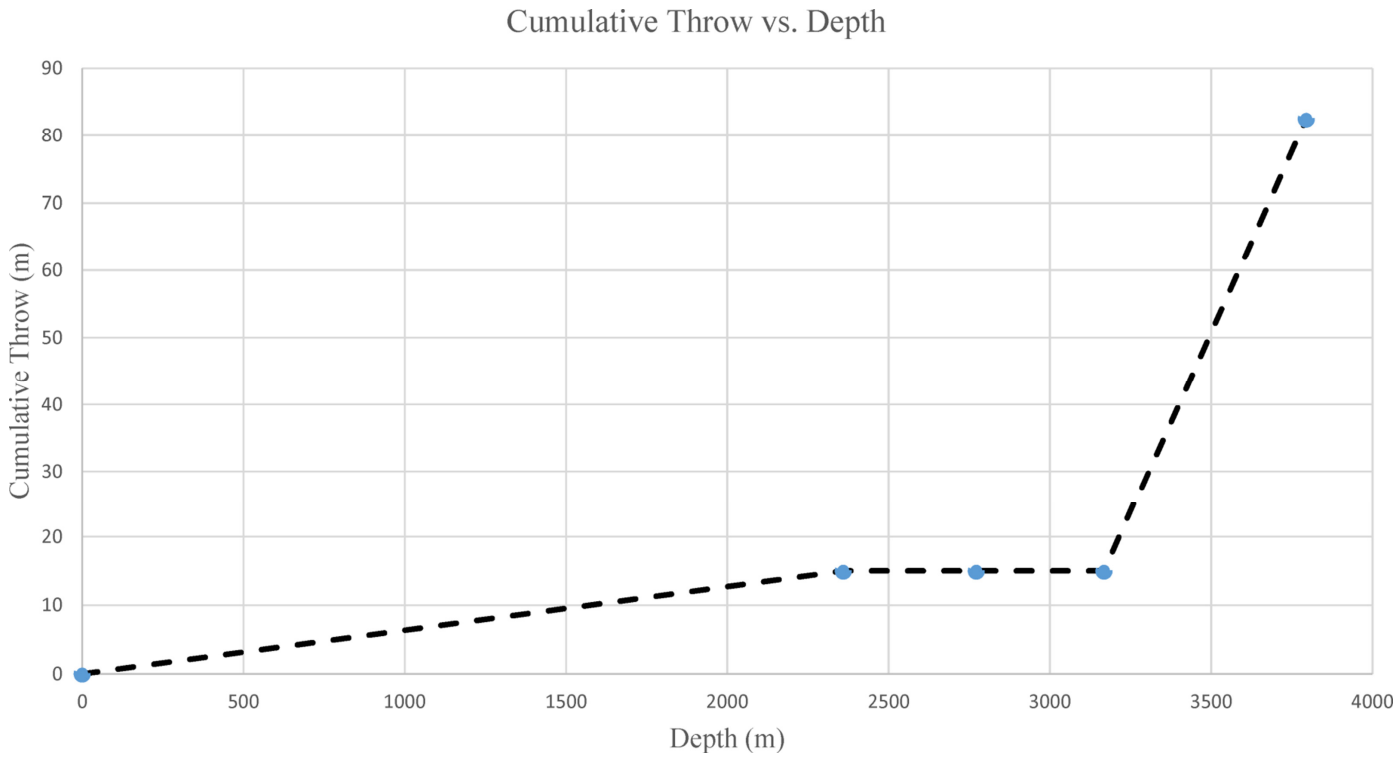

Figure 6. T–Z plot for fault 2 along regional cross-section C-C' (Appendix) showing cumulative throw of ~82.5 m. Zero slope between interpolated points represents periods of fault inactivity. Dots represent values of cumulative throw and depth of formation tops in the hanging-wall block.

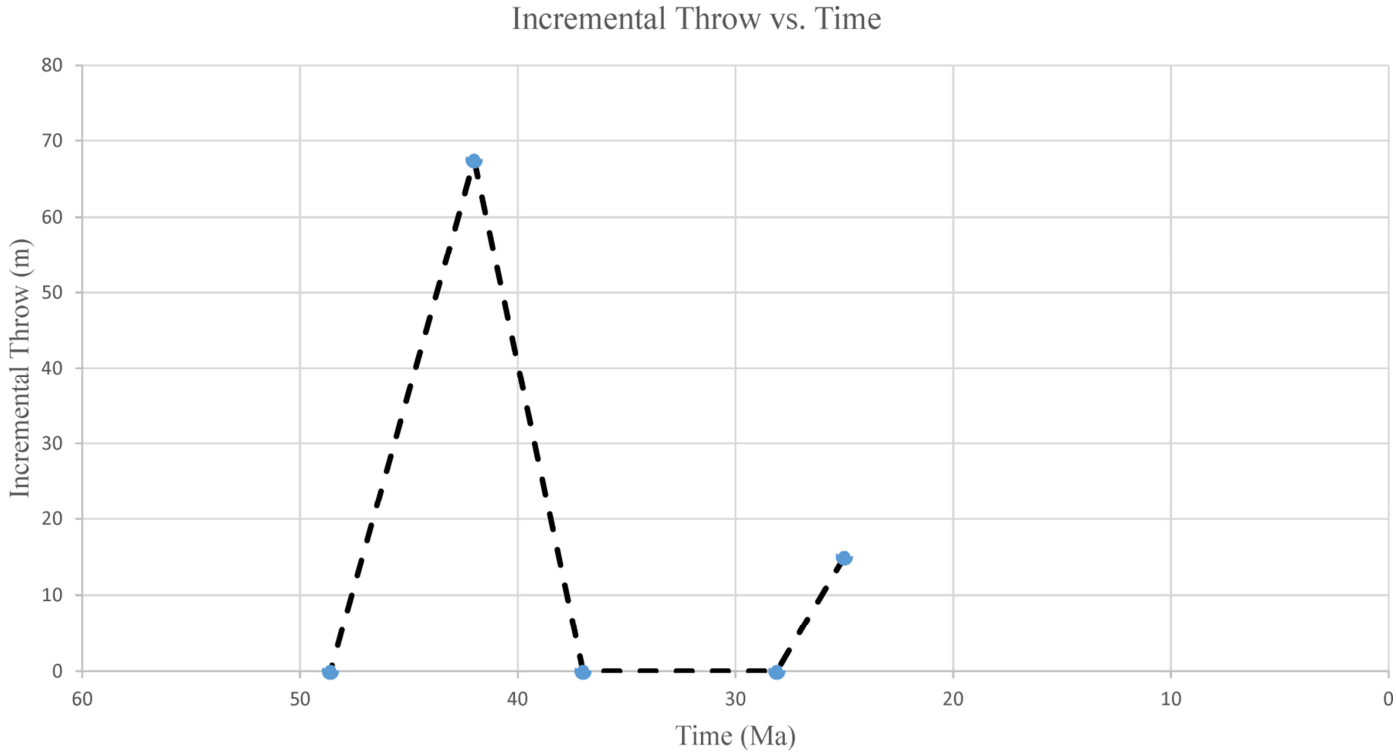

Figure 7. ΔT–t plot for the same fault in Figure 6 above showing no increase in throw from the Eocene-Oligocene (42–25 Ma). Maximum incremental throw of ~68 m also occurs during the Eocene.

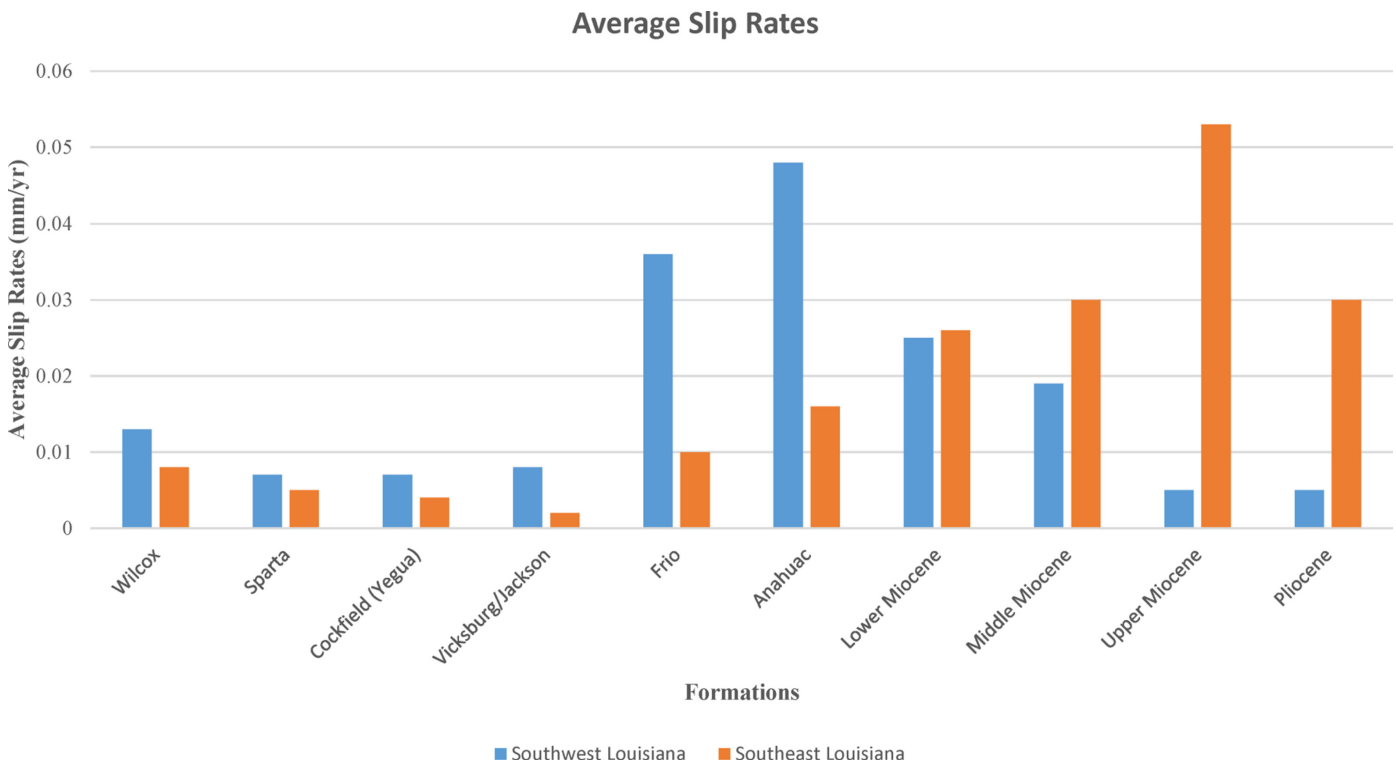

Figure 8. Average slip rates of sedimentary units (Fig. 3) for southwestern and southeastern Louisiana. Notice the shift in relatively higher slip rates from the west to the east in southern Louisiana beginning in the Early Miocene.

Table 1. Average slip rates for all 11 regional cross sections. See Appendix for number of faults in each cross section (Fig. 2).

	Southwestern Louisiana (A–A' through F–F')							Southeastern Louisiana (M–M' through Q–Q')				
	A–A'	**B–B'**	**C–C'**	**D–D'**	**E–E'**	**F–F'**		**M–M'**	**N–N'**	**O–O'**	**P–P'**	**Q–Q'**
Pliocene	0	0	0	0	0	0.005		0.051	0.016	0.027	0	0
Upper Miocene	0	0	0	0.002	0	0.008		0.029	0.013	0.087	0.098	0.04
Middle Miocene	0.041	0.017	0.013	0.007	0.012	0.023		0.014	0.019	0.038	0.058	0.023
Lower Miocene	0.025	0.074	0.014	0.01	0.008	0.022		0.013	0.004	0.042	0.033	0.036
Anahuac	0.057	0.069	0.044	0.016	0.048	0.051		0.02	0.033	0	0	0.028
Frio	0.013	0.093	0.017	0.017	0.029	0.045		0	0.006	0.019	0	0.005
Vicksburg/ Jackson	0.001	0.013	0.003	0.006	0.012	0.015		0	0.003	0.002	0	0.001
Cockfield (Yegua)	0.005	0.008	0.009	0.005	0.014	0.008		0	0.007	0	0	0.002
Sparta	0.003	0.006	0.008	0.007	0.005	0.008		0	0.01	0.005	0.002	0.002
Wilcox	0	0	0	0.004	0.021	0.061		0	0	0.013	0	0.002

maximum cumulative throw across a particular formation top tends to increase along the different faults in a basinward direction (Appendix).

Calculated incremental throw and average fault slip rates show the maximum slip rate in the Late Miocene (Tables 1 and 3; Fig. 8; Appendix), however the stratigraphy displayed in the well logs does not sample the Pliocene and younger sediments making it difficult to constrain the incremental throw to this time because without younger sediments we cannot determine if the throw is cumulative or a single increment. Calculated average sedimentation rates show maximum values during the Middle Miocene (Table 2). These maximum slip rates and sedimentation rates represent relatively high values for the Gulf Coast.

DISCUSSION

The salt tectonics model (Vendeville, 2005) predicts that the timing of sedimentation should correlate with the timing of fault activity and salt movement. In addition, salt structures within the sedimentary sequence may provide further evidence for syn-depositional salt movement.

The incremental throw increases five-fold in the Late Oligocene to Early Miocene during the emergence of a fluvial dominated deltaic depositional center (Red River axis) in southwestern Louisiana in addition to a shift in the Mississippi River fluvial dominated deltaic system from southcentral Louisiana toward the southwest (Galloway et al., 2000, 2011) (Figs. 1 and 8; Appen-

Table 2. Average sedimentation rates for all 11 regional cross sections (Fig. 2).

	Southwestern Louisiana (A–A' through F–F')							Southeastern Louisiana (M–M' though Q–Q')				
	A–A'	B–B'	C–C'	D–D'	E–E'	F–F'		M–M'	N–N'	O–O'	P–P'	Q–Q'
Pliocene	0	0	0	0	0	0		0	0.58	0	0	0
Upper Miocene	0	0	0	0.093	0.075	0.107		0.163	0.257	0.247	0.226	0.291
Middle Miocene	0.223	0.222	0.269	0.27	0.349	0.321		0.426	0.495	0.424	0.307	0.267
Lower Miocene	0.135	0.165	0.133	0.217	0.125	0.175		0.125	0.106	0.12	0.099	0.138
Anahuac	0.323	0.25	0.205	0.31	0.169	0.192		0.222	0.219	0.12	0.159	0.171
Frio	0.434	0.313	0.405	0.325	0.295	0.314		0.172	0.171	0.152	0.126	0.087
Vicksburg/ Jackson	0.064	0.074	0.072	0.081	0.072	0.054		0.017	0.029	0.011	0.01	0.009
Cockfield (Yegua)	0.172	0.137	0.121	0.115	0.126	0.089		0.035	0.051	0.046	0.052	0.05
Sparta	0.079	0.104	0.12	0.108	0.114	0.11		0.048	0.048	0.031	0.025	0.028
Wilcox	0	0	0.138	0.157	0.155	0.147		0	0	0	0	0

Table 3. Average slip rates and Incremental throw for southwestern and southeastern Louisiana.

	Southwestern Louisiana		Southeastern Louisiana	
	Slip rates (mm/yr)	Incremental Throw (m)	Slip rates (mm/yr)	Incremental Throw (m)
Pliocene	0.005	15	0.032	86.2
Upper Miocene	0.005	31.9	0.053	336.0
Middle Miocene	0.019	82.8	0.031	133.2
Lower Miocene	0.025	180.0	0.026	180.2
Anahuac	0.048	93.7	0.016	31.8
Frio	0.036	110.4	0.01	31.2
Vicksburg/Jackson	0.008	72.5	0.002	17.5
Cockfield (Yegua)	0.007	37.4	0.004	20.6
Sparta	0.007	44.3	0.005	30.0
Wilcox	0.013	133.8	0.008	80.6

dix; Tables 1 and 3). The shift in the depositional center location records the westernmost shift in deposition from the center of the southern Louisiana portion of the northern Gulf Coast margin in the Cenozoic.

In southeastern Louisiana, during the Early Miocene, incremental throw increases six-fold over the previous values. The Early Miocene increase correlates with the time when the fluvial depositional axis and center began to shift eastward and a new depositional axis, the Tennessee River depositional axis, emerged (Galloway et al., 2000, 2011) (Figs. 1 and 8; Appendix; Tables 1 and 3). The incremental throw and slip rates increase in southeastern Louisiana from this time until the Late Miocene and then decrease in the Pliocene. However, the Pliocene slip rates (0.032 mm/yr) are significantly higher than the relatively lower Eocene-Oligocene rates (0.007–0.016 mm/yr) (Tables 1 and 3; Appendix).

To study further the correlation between the timing of fault activity and the timing of sediment deposition and salt movement, the fault activity between southwestern and southeastern Louisiana are compared (Fig. 8). A comparison between the slip rates and incremental throw in southwestern and southeastern Louisiana (Tables 1 and 3; Fig. 8) conforms to the pattern of a shift in the depositional center from the west to the east in the Cenozoic. From the Paleocene to the Early Miocene, the slip rates and incremental throw in southwestern Louisiana are 1.5–3.5 times greater than those of the southeast. In the Early Miocene, the slip rates and incremental throw are approximately the same between southwestern and southeastern Louisiana and are 1.5–10 times higher in the southeast between the Early Miocene and Pliocene.

The resulting local sedimentation rates (Table 2) calculated from decompacted sediment thicknesses could not be used effectively in this study because they do not show a correlation with the slip rates at all times in the Cenozoic possibly due to inadequate data. Proper correlation with older, more deeply buried sediments was not possible because along some parts of the cross sections these sediments were not penetrated by the well logs. As a result, incremental throw values could not be calculated along these parts of the cross sections leaving insufficient values available to calculate the average values for the time periods represented by the sediments. Southward of the cross section, faulting is expected to increase in the direction of the depositional center (Murray, 1961; Winker, 1982). Older, deeper, unpenetrated sediments with higher sedimentation rates may show larger slip rates and incremental throw that will then reflect in the average rates calculated for that time period. However, along individual faults incremental throw magnitudes correlate with sedimentation rates.

Periods of fault inactivity mainly occur during the Eocene, a time when the depositional center was located in central Louisi-

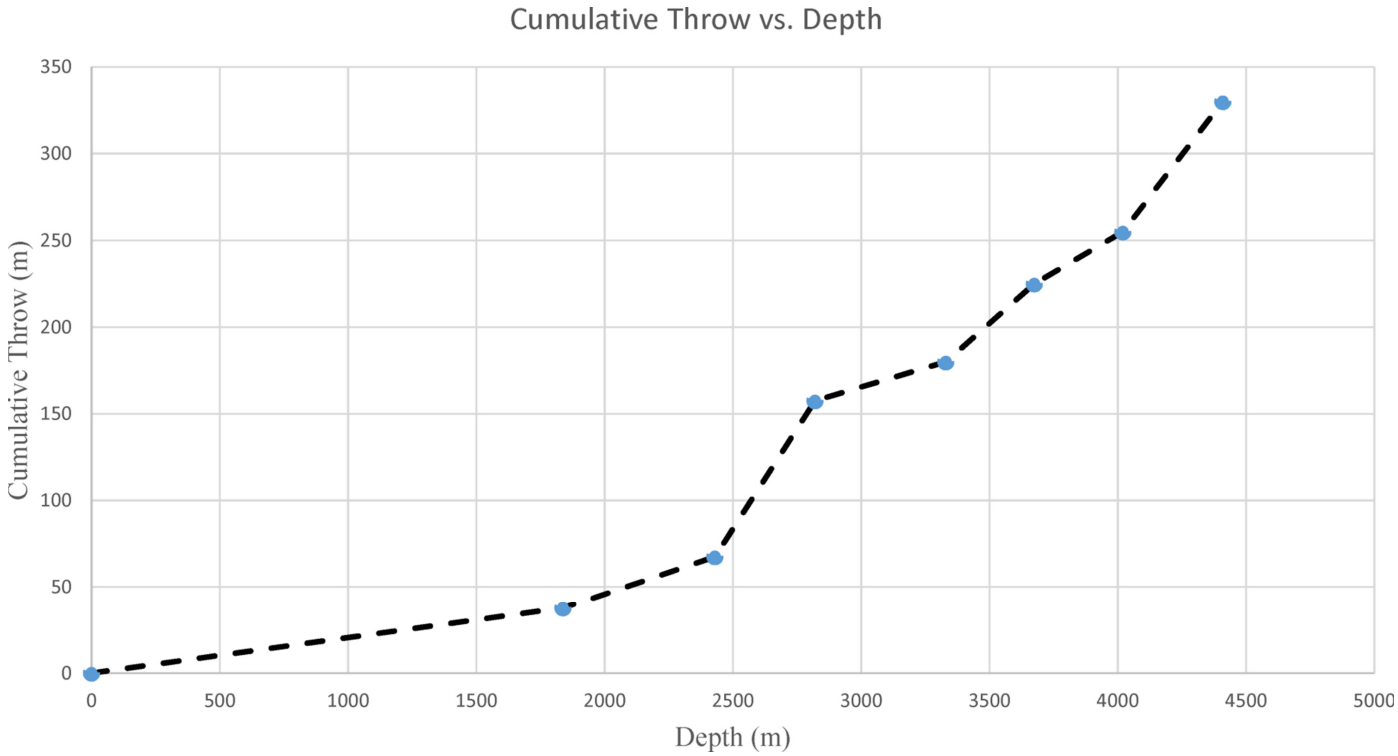

Figure 9. T–Z plot for fault 2 along regional cross-section N–N' (Appendix) showing cumulative throw of 330 m. Positive slopes indicate continuous fault reactivation. Dots represent values of cumulative throw and depth of formation tops in the hanging-wall block.

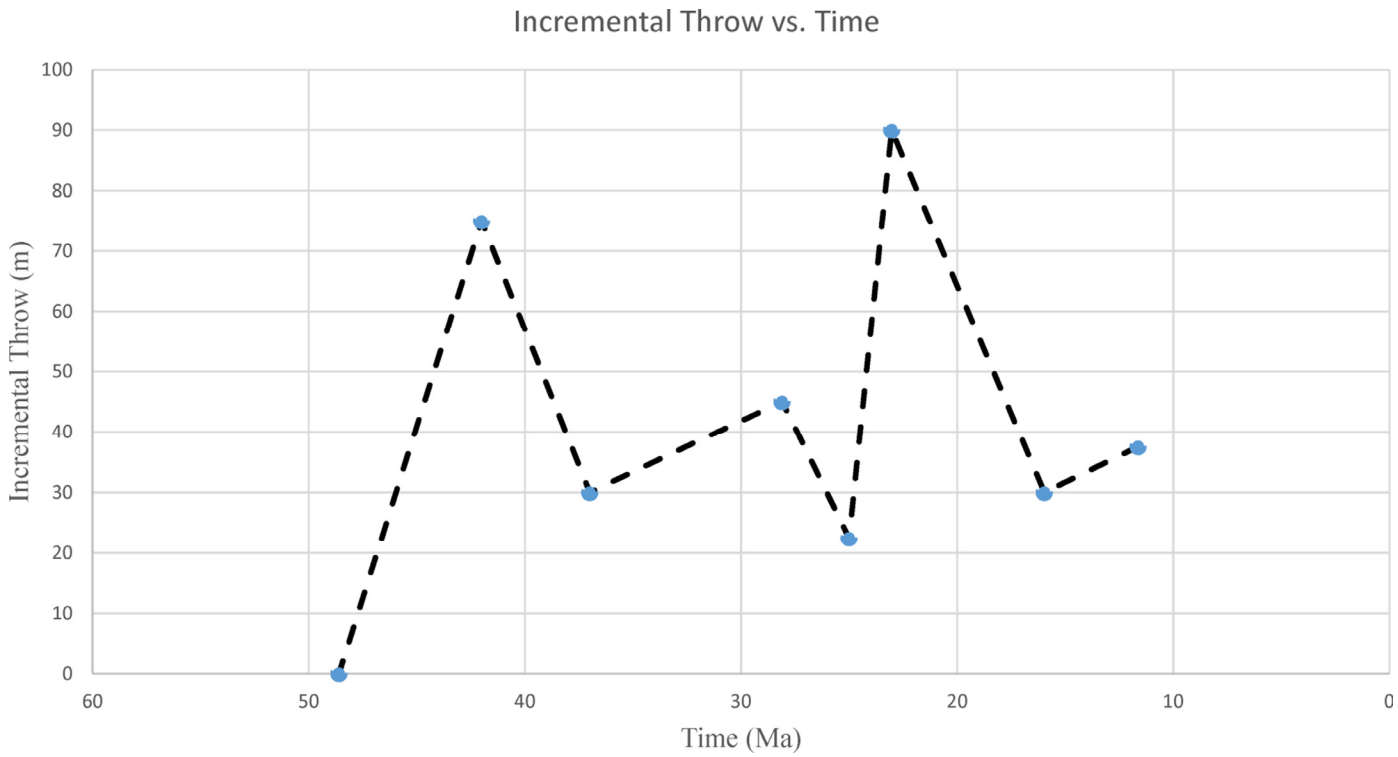

Figure 10. ΔT–t plot for the same fault in Figure 9 above showing an overall increase in throw from the Eocene through Miocene (49–12 Ma). Maximum incremental throw of ~90 m along the fault in the Lower Miocene.

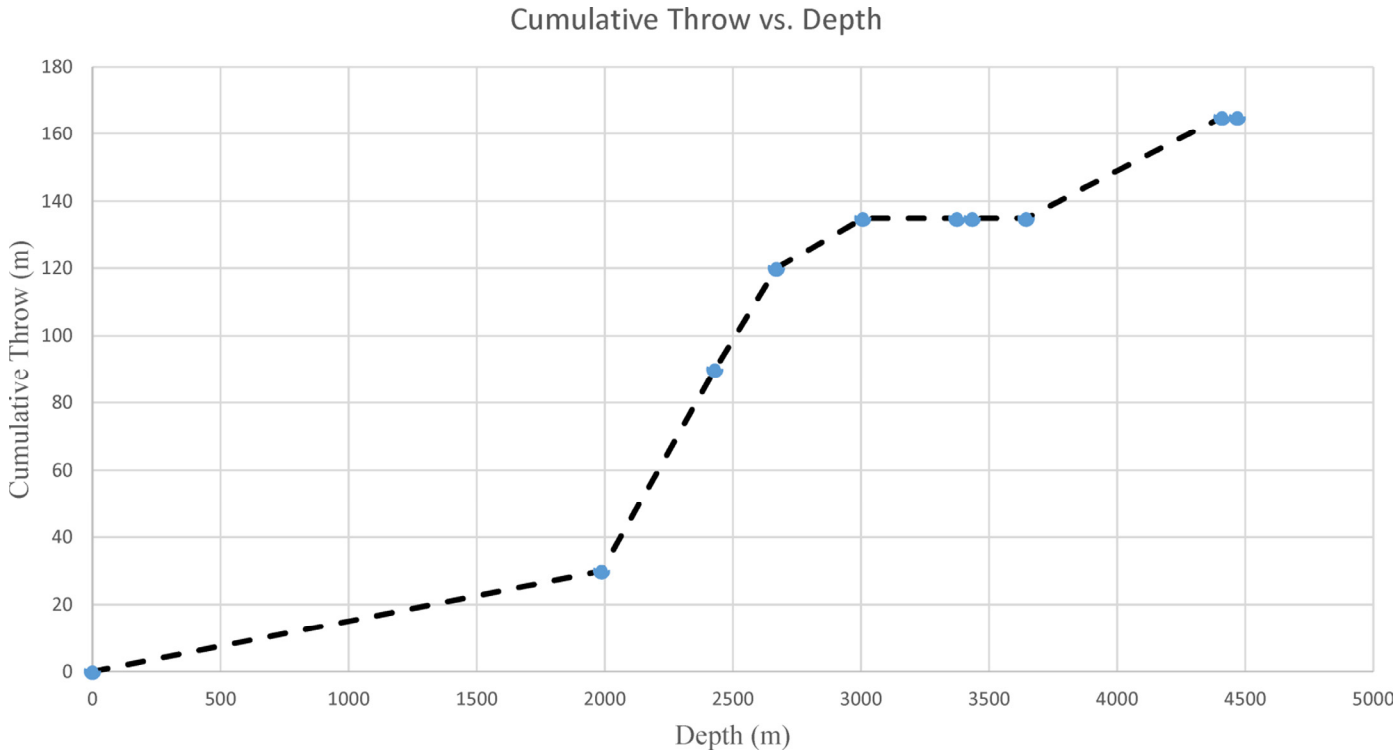

Figure 11. T–Z plot for fault 2 along regional cross-section Q–Q' (Appendix) showing cumulative throw of 165 m. Zero slopes between interpolated points indicates periods of inactivity between periods fault reactivation. Dots represent values of cumulative throw and depth of formation tops in the hanging-wall block.

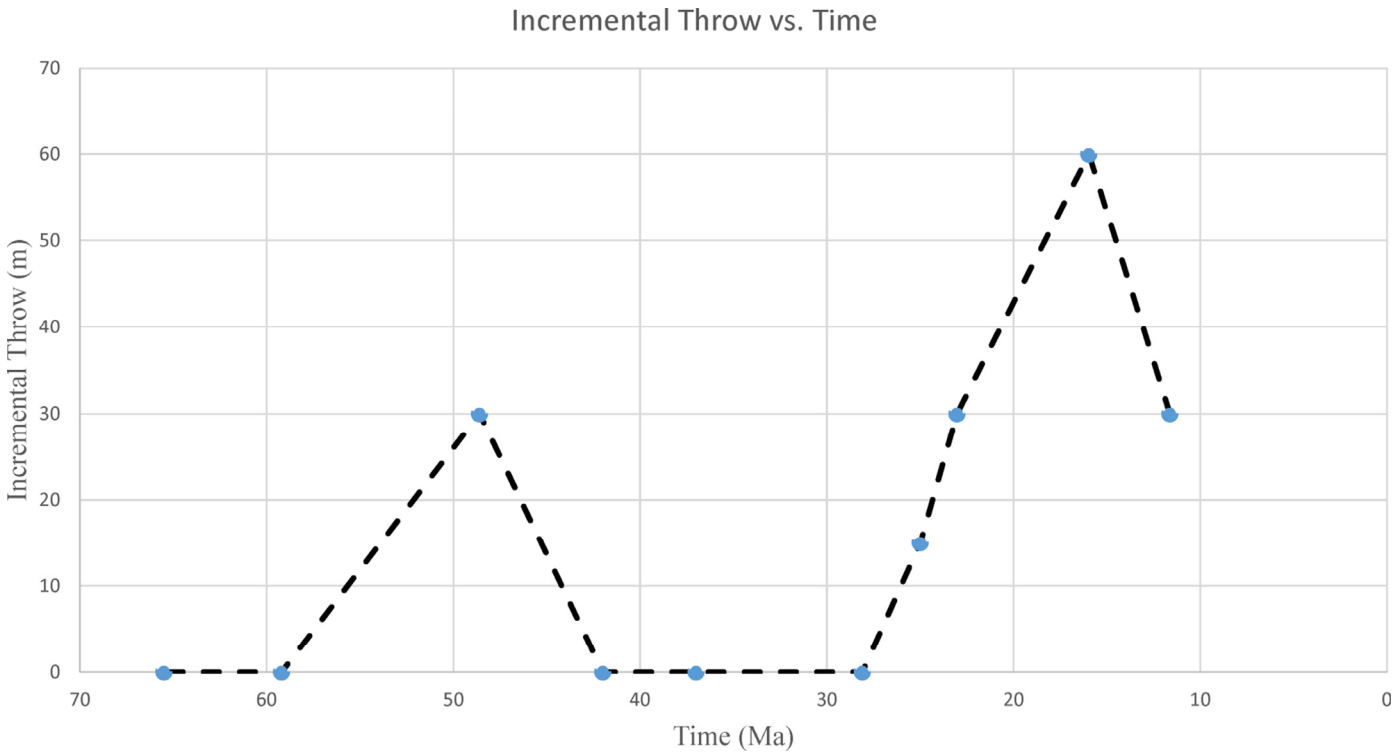

Figure 12. ΔT–t plot for the same fault in Figure 11 above showing increase in throw punctuated by periods of inactivity in the Eocene (48.6–25 Ma). Maximum incremental throw of ~60 m in the Middle Miocene.

ana. The Eocene is a time of relatively low sedimentation rate and coastal retreat (Galloway et al., 2011).

Within the regional cross sections, there are ten notable salt structures (Fig. 2) some of which pierce the youngest sediments. The salt diapirs that pierce the sediments suggest vertical salt displacement from differential loading or gravity spreading. Relatively high differences in sediment thickness and incremental throw magnitude also occur on the flanks of these salt structures suggesting syn-depositional salt movement. Salt piercement structures are more consistent with differential loading and gravity spreading models (Vendeville, 2005).

Observations in this study show that in southwestern Louisiana, normal faulting is most active during the Paleocene-Eocene and the Oligocene–Early Miocene time, and in contrast, in southeastern Louisiana faulting is relatively more active during the Early Miocene to Late Miocene. During these most active periods, salt movement is associated with faulting and sediment loading using model predictions of an updip extension zone, a middle translation zone and a downdip (basinward) contraction zone observed from salt and sediment stratigraphy and structure in seismic sections from southwestern and southeastern Louisiana (Diegel et al., 1995; McBride, 1998). Offshore southwestern and southeastern Louisiana are fold belts associated with the downdip contraction formed by the evacuation of salt from onshore updip areas of extension in southwestern Louisiana (Diegel et al., 1995) and southeastern Louisiana (McBride, 1998).

The results of this study support the model for fault development by salt movement via differential loading or gravity spreading over the lithospheric flexure model in the Cenozoic. The lithospheric flexure model predicts that the tensional stresses that induce faulting occur on the periphery of the loading zone. Although the depositional center in the Pliocene is offshore (Fig. 1) and faulting should be expected onshore in southeastern Louisiana, significant slip rates and incremental throw are not observed across faults onshore in the Pliocene except in the three cross sections where prominent salt piercement structures exist.

The calculated slip rates and incremental throw in this study represent values of minimum fault-related subsidence rates for southern Louisiana in the Paleocene-Pliocene. Together with sedimentation rates, these subsidence rates can be compared with Pleistocene–present day sedimentation rates and slip rates to further understand sedimentation-related fault activity associated with ancient and modern river systems in southern Louisiana. This can provide important considerations for future sustainability by allowing for predictions of rates of coastal land loss and planning for preventive measures. The results of this study also imply that future subsidence may be expected in areas of sediment deposition where there is salt at depth.

This study is subject to some limitations and errors. The well logs in the study do not sample depths shallower than 3000 ft. so that the Pliocene is not sampled in three of the regional cross sections (A–A', B–B', and C–C') from southwestern Louisiana. As well, the top of the Pliocene/base of the Pleistocene is only sampled in one cross section.

However, in the eight cross sections that sampled the Pliocene sediments allowed for a correlation and comparison between the fault activity and salt movement in both southwestern and southeastern Louisiana during the Cenozoic because fault throw is measured from the bottom of the stratigraphic interval in the footwall and hanging-wall blocks. The calculated errors in the measurement of the cumulative throw from which incremental throw and slip rate values were calculated is approximately five percent. Additional error may result in slip rates because the numerical ages used in calculating slip rates represent published ages recorded for particular formations in southern Louisiana, however the deposition of the formation in the cross section may not have spanned the entire period and as such would result in higher slip rates/subsidence rates. Overpressuring can cause weakness in sediments and increase susceptibility to faulting (Dugan and Sheahan, 2012). The Gulf Coast Tertiary sediments are known to be overpressured in some areas; this may further influence fault activity outside model predictions of salt displacement and lithospheric flexure.

CONCLUSIONS

Faults have been reactivated in southern Louisiana throughout the Cenozoic. Periods of fault reactivation are punctuated by periods of fault inactivity. Faulting along the coastal plain of southern Louisiana is sensitive to changes in depositional center location. The slip rates and incremental throw magnitude increases five to six times over previous amounts in space and time concomitant with the emergence of deltaic depositional centers in southwestern and southeastern Louisiana. In addition, the periods of inactivity and low fault slip rates are mostly constrained to the period when the depositional center moved away and the area experienced minimal sediment input. Furthermore, the amount and timing of faulting differs between southwestern and southeastern Louisiana in a pattern reflective of the spatial and temporal changes in sediment deposition between these areas. This correlative pattern between sediment deposition and fault reactivation is marked by a shift in the major activity from the west to the east in southern Louisiana in the Cenozoic.

The timing of fault activity correlates with the timing of salt movement suggesting salt movement via differential loading or gravity spreading. The interaction among fault activity, sediment deposition and salt movement are consistent with model predictions of fault initiation and reactivation due to sediment induced salt displacement in contrast to model predictions of fault activity due to lithospheric flexure.

Future analysis of faults in south-central Louisiana may provide further verification of the interaction among major fault activity, sediment deposition and salt displacement described in this study. Structural and stratigraphic studies of Pleistocene and Holocene sediments is recommended, as this will provide data to aid in defining the relationship between ancient and modern systems. The role of overpressuring in fault activity should be considered in greater detail than in this current study because Tertiary Gulf Coast sediments are known to be overpressured. Finally, these faults hold a record of the interaction among climate, tectonics, sediment deposition and salt movement and should be further studied in this regard.

REFERENCES CITED

Al Dhamen, Ali A., 2014, Fault kinematics along the coastal plain of South Louisiana: Implications for tectono-climatic-induced deformation along a passive continental margin: M.S. Thesis, Louisiana State University, Baton Rouge, 50 p.

Allen, P., and J. R. Allen, 2006, Basin analysis. Principles and application to petroleum play assessment: Blackwell Scientific Publications, Oxford, U.K., 549 p.

Bebout, D. G., and D. R. Gutiérrez, 1982, Regional cross sections, Louisiana Gulf Coast: Western part: Louisiana Geological Survey Folio Series 5, Baton Rouge, 11 p.

Bebout, D. G., and D. R. Gutiérrez, 1983, Regional cross sections, Louisiana Gulf Coast: Eastern part: Louisiana Geological Survey Folio Series 6, Baton Rouge, 10 p.

Cartwright, J., R. Bouroullec, D. James, and H. Johnson, 1998, Polycyclic motion history of some Gulf Coast growth faults from high-resolution displacement analysis: Geology, v. 26, p. 819–822.

Castelltort, S., S. Pochat, and J. Van Den Driessche, 2004, Using T–Z plots as a graphical method to infer lithological variations from growth strata: Journal of Structural Geology, v. 26, p. 1425–1432.

Combellas-Bigott, R. I., and W. E. Galloway, 2006, Depositional and structural evolution of the middle Miocene depositional episode, east-central Gulf of Mexico: American Association of Petroleum Geologists Bulletin, v. 90, p. 335–362.

Diegel, F. A., J. Karlo, D. Schuster, R. Shoup, and P. Tauvers, 1995, Cenozoic structural evolution and tectono-stratigraphic framework of the northern Gulf Coast continental margin, *in* M. P. A. Jackson, D. G. Roberts, and S. Snelson, eds., Salt tectonics: A global perspective: American Association of Petroleum Geologists Memoir 65, Tulsa, Oklahoma, p. 109–151.

Dugan, B., and T. Sheahan, 2012, Offshore sediment overpressures of passive margins: Mechanisms, measurement, and models: Reviews of Geophysics, v. 50, Paper RG3001, 20 p.

Galloway, W. E., P. E. Ganey-Curry, X. Li, and R. T. Buffler, 2000, Cenozoic depositional history of the Gulf of Mexico Basin: American Association of Petroleum Geologists Bulletin, v. 84, p. 1743–1774.

Galloway, W. E., T. L. Whiteaker, and P. Ganey-Curry, 2011, History of Cenozoic North American drainage basin evolution, sediment yield, and accumulation in the Gulf of Mexico Basin: Geosphere, v. 7, p. 938–973.

Hackley, P. C., 2012, Geologic assessment of undiscovered conventional oil and gas resources—Middle Eocene Claiborne Group, United States part of the Gulf of Mexico Basin: U.S. Geological Survey Open-File Report 2012–1144, 87 p., <http://pubs.usgs.gov/of/2012/1144/> Last accessed August 20, 2015.

Hanor, J. S., 1982, Reactivation of fault movement, Tepetate Fault Zone, south central Louisiana: Gulf Coast Association of Geological Societies Transactions, v. 32, p. 237–245.

Heinrich, P., 2000, The De Quincy fault-line scarp: Beauregard and Calcasieu parishes, Louisiana: Basin Research Institute Bulletin, v. 9, p. 38–50.

Kusznir, N.J., A. M. Roberts, and C. K. Morley, 1995, Forward and reverse modelling of rift basin formation, in J. J. Lambiase, ed., Hydrocarbon habitat in rift basins: Geological Society of London Special Publications, v. 80, p. 33–56.

Lopez, J. A., 1990, Structural styles of growth faults in the U.S. Gulf Coast Basin: Geological Society of London Special Publications, v. 50, p. 203–219.

Mansfield, C., J. and Cartwright, 1996, High resolution fault displacement mapping from three-dimensional seismic data: Evidence for dip linkage during fault growth: Journal of Structural Geology, v. 18, p. 249–263.

McBride, B. C., 1998, The evolution of allochthonous salt along a megaregional profile across the northern Gulf of Mexico Basin: American Association of Petroleum Geologists Bulletin, v. 82, p. 1037–1054.

Nunn, J. A., 1985, State of stress in the northern Gulf Coast: Geology, v. 13, p. 429–432.

Peel, F. J., C. J. Travis, and J. R. Hossack, 1995, Genetic structural provinces and salt tectonics of the Cenozoic offshore U.S. Gulf of Mexico: A preliminary analysis, *in* M. P. A. Jackson, D. G. Roberts, and S. Snelson, eds., Salt tectonics: A global perspective: American Association of Petroleum Geologists Memoir 65, Tulsa, Oklahoma, p. 153–175.

Schuster, D., 1995, Deformation of allochthonous salt and evolution of related salt-structural systems, eastern Louisiana Gulf Coast, *in* M. P. A. Jackson, D. G. Roberts, and S. Snelson, eds., Salt tectonics: A global perspective: American Association of Petroleum Geologists Memoir 65, Tulsa, Oklahoma, p. 177–198.

Thorsen, C., 1963, Age of growth faulting in southeast Louisiana: Gulf Coast Association of Geological Societies Transactions, v. 13, p. 103–110.

Tearpock, D. J., and R. E. Bischke, 2003, Applied subsurface geological mapping: With structural methods: Prentice Hall, Upper Saddle River, New Jersey, 822 p.

Vendeville, B. C., 2005, Salt tectonics driven by sediment progradation: Part I—Mechanics and kinematics: American Association of Petroleum Geologists Bulletin, v. 89, p. 1071–1079.

Winker, C. D., 1982, Cenozoic shelf margins, northwestern Gulf of Mexico Basin: Gulf Coast Association of Geological Societies Transactions, v. 32, p. 427–448.

Woodbury, H., I. Murray, Jr., P. Pickford, and W. Akers, 1973, Pliocene and Pleistocene depocenters, outer continental shelf, Louisiana and Texas: American Association of Petroleum Geologists Bulletin, v. 57, p. 2438–2439.

Worrall, D., and S. Snelson, 1989, Evolution of the northern Gulf of Mexico, *in* A. W. Bally and A. R. Palmer, eds., The geology of North America, v. A: An overview: Geological Society of America, Boulder, Colorado, p. 97–138.

APPENDIX

Incremental Throw from Cross-Sections A–A' though F–F' (Southwestern Louisiana) and M–M' through Q–Q' (Southeastern Louisiana).

Incremental throw (ΔT in meters) for cross-section A–A'.

	1	2	3	4	5	6	7	8	9	10	11	12	13	14	15
Upper Miocene															
Middle Miocene															60
Lower Miocene										15	38	83	60	195	120
Anahuac										68	120	98	75	120	
Frio					23	15	0	30	45	83					
Vicksburg/Jackson			15	15	0	0	15	15	23						
Cockfield (Yegua)			15	23	0	8	45	45							
Sparta	68	38	0	0	0	8	30	98							
Wilcox															

Incremental throw (∆T in meters) for cross-section B–B'.

	1	2	3	4	5	6	7	8	9	10	11
Upper Miocene											
Middle Miocene										75	
Lower Miocene									1035	285	248
Anahuac									135		
Frio							37.5	540			
Vicksburg/Jackson				60	120	135	15	240			
Cockfield (Yegua)		15	30	7.5	22.5	150	7.5				
Sparta	30	75	22.5	7.5	7.5		90				
Wilcox	45										
Midway	7.5										

Incremental throw (∆T in meters) for cross-section C–C'.

	1	2	3	4	5	6	7	8	9	10	11	12	13
Upper Miocene													
Middle Miocene												22.5	90
Lower Miocene					22.5	15	30	90	60	150	375	52.5	75
Anahuac	15				30	7.5	172.5	0	75	30	345	15	
Frio	22.5	15	15	7.5	37.5	60	217.5						
Vicksburg/Jackson	15	0	0	7.5	60	37.5							
Cockfield (Yegua)	22.5	0	0	7.5	90	60							
Sparta	30	67.5	45	67.5	30								
Wilcox													

Incremental throw (∆T in meters) for cross-section D–D'.

	1	2	3	4	5	6	7	8	9	10	11	12	13	14
Upper Miocene												15		
Middle Miocene										15	15	15	67.5	45
Lower Miocene						60	60	67.5	90	120	45			
Anahuac						15	15	22.5	75					
Frio		30	22.5		97.5	45	75							
Vicksburg/Jackson	30	7.5	60	105	52.5									
Cockfield (Yegua)	0	22.5	37.5	15										
Sparta	52.5	45	0	60										
Wilcox		30	52.5											

Incremental throw (∆T in meters) for cross-section E–E'.

	1	2	3	4	5	6	7	8	9	10	11	12	13
Upper Miocene													
Middle Miocene					15	60	22.5	30	150	45	75	30	30
Lower Miocene			30	30	30	97.5	22.5	0	195	52.5	60	60	
Anahuac	60		112.5	15	7.5	157.5	120	345		37.5			
Frio	7.5	15	45	135	247.5								
Vicksburg/Jackson	15	30	247.5	135									
Cockfield (Yegua)	37.5	15	150										
Sparta	75	7.5	15										
Wilcox	225												

Incremental throw (∆T in meters) for cross-section F–F'.

	1	2	3	4	5	6	7	8	9	10
Pliocene										
Upper Miocene										
Middle Miocene										37.5
Lower Miocene					187.5	112.5	97.5	135	120	37.5
Anahuac	15	0	15	0	22.5	15	7.5	30	15	52.5
Frio	15	15	22.5	15	15	532.5	270	135	225	
Vicksburg/Jackson	0	0	7.5	90	390	300				
Cockfield (Yegua)	22.5	0	0	30	150					
Sparta	7.5	60	30	30	112.5					
Wilcox	135									

Incremental throw (∆T in meters) for cross-section F–F' (continued).

	11	12	13	14	15	16	17	18	19	20
Pliocene									15	15
Upper Miocene				22.5		52.5	75	97.5	30	30
Middle Miocene			210	60	165	150	127.5	67.5	30	60
Lower Miocene	37.5	37.5	570	97.5	22.5	270	270			
Anahuac	22.5	202.5	697.5							
Frio										
Vicksburg/Jackson										
Cockfield (Yegua)										
Sparta										
Wilcox										

Incremental throw (∆T in meters) for cross-section M–M'.

	1	2	3	4	5	6	7	8	9	10	11	12	13	14
Pliocene						67.5	90	15	7.5		127.5	195	90	525
Upper Miocene						97.5	30	0	22.5	345	262.5	435	15	420
Middle Miocene	30	30	52.5	45	45	120		90	135					
Lower Miocene	30	30	67.5	120	105	195								
Anahuac	45	60	7.5	45										
Frio														
Vicksburg/Jackson														
Cockfield (Yegua)														
Sparta														

Incremental throw (∆T in meters) for cross-section N–N'.

	1	2	3	4	5	6	7	8	9
Pliocene						15	52.5	15	15
Upper Miocene				30	30	15	37.5	15	15
Middle Miocene		37.5	15	15	105	45	120	45	45
Lower Miocene	22.5	30	0	15	75				
Anahuac	7.5	90	15	60	150				
Frio	15	22.5							
Vicksburg/Jackson	15	45							
Cockfield (Yegua)	37.5	30							
Sparta	52.5	75							

Incremental throw (∆T in meters) for cross-section N–N' (continued).

	10	11	12	13	14	15	16	17
Pliocene	30	15	45	15	60	105	90	67.5
Upper Miocene	52.5	15	15		75	375	180	172.5
Middle Miocene	202.5	180						
Lower Miocene								
Anahuac								
Frio								
Vicksburg/Jackson								
Cockfield (Yegua)								
Sparta								
Wilcox								

Incremental throw (∆T in meters) for cross-section O–O'.

	1	2	3	4	5	6	7
Pliocene							75
Upper Miocene						90	1005
Middle Miocene		60	120	75	405		
Lower Miocene	180	157.5	555				
Anahuac	0						
Frio	60						
Vicksburg/Jackson	15						
Cockfield (Yegua)	0						
Sparta	30						
Wilcox	135						

Incremental throw (∆T in meters) for cross-section P–P'.

	1	2	3	4	5	6	7	8
Upper Miocene						90	1395	367.5
Middle Miocene			360	202.5	195			
Lower Miocene	255	210						
Anahuac	0							
Frio	0							
Vicksburg/Jackson	0							
Cockfield (Yegua)	0							
Sparta	15							
Wilcox								

Incremental throw (∆T in meters) for cross-section Q–Q'.

	1	2	3	4	5	6	7
Upper Miocene	0	0	0	0	0	60	450
Middle Miocene	22.5	30	157.5	75	210		
Lower Miocene	37.5	60	22.5	885			
Anahuac	15	30	120				
Frio	15	15	15				
Vicksburg/Jackson	15	0					
Cockfield (Yegua)	15	0					
Sparta	22.5	0					
Wilcox	22.5	30					
Midway	15	0					